Journal of Alzheimer's Disease 43 (2015) 1343–1353
DOI 10.3233/JAD-141074
IOS Press

Lower Brain ^{18}F-Fluorodeoxyglucose Uptake But Normal ^{11}C-Acetoacetate Metabolism in Mild Alzheimer's Disease Dementia

Christian-Alexandre Castellano[a,b,*], Scott Nugent[a,b], Nancy Paquet[c], Sébastien Tremblay[d], Christian Bocti[a,c], Guy Lacombe[a,e], Hélène Imbeault[a], Éric Turcotte[c,d], Tamas Fulop[a,e] and Stephen C. Cunnane[a,e]
[a]*Research Center on Aging, Health and Social Sciences Center, Geriatrics Institute, Sherbrooke, QC, Canada*
[b]*Department Physiology and Biophysics, Université de Sherbrooke, Sherbrooke, QC, Canada*
[c]*Department of Nuclear Medicine and Radiobiology, Université de Sherbrooke, Sherbrooke, QC, Canada*
[d]*Sherbrooke Molecular Imaging Center, Université de Sherbrooke, Sherbrooke, QC, Canada*
[e]*Department of Medicine, Université de Sherbrooke, Sherbrooke, QC, Canada*

Handling Associate Editor: David Knopman

Accepted 30 July 2014

Abstract.
Background: The cerebral metabolic rate of glucose (CMRg) is lower in specific brain regions in Alzheimer's disease (AD). The ketones, acetoacetate and β-hydroxybutyrate, are the brain's main alternative energy substrates to glucose.
Objective: To gain insight into brain fuel metabolism in mild AD dementia by determining whether the regional CMR and the rate constant of acetoacetate (CMRa and Ka, respectively) reflect the same metabolic deficit reported for cerebral glucose uptake (CMRg and Kg).
Methods: Mild AD dementia (Mild AD; $n = 10$, age 76 y) patients were compared with gender- and age-matched cognitively normal older adults (Controls; $n = 29$, age 75 y) using a PET/MRI protocol and analyzed with both ROI- and voxel-based methods.
Results: ROI-based analysis showed 13% lower global CMRg in the gray matter of mild AD dementia versus Controls (34.2 ± 5.0 versus 38.3 ± 4.7 μmol/100 g/min, respectively; $p = 0.015$), with CMRg and Kg in the parietal cortex, posterior cingulate, and thalamus being the most affected ($p \leq 0.022$). Neither global nor regional CMRa or Ka differed between the two groups (all $p \geq 0.188$). Voxel-based analysis showed a similar metabolic pattern to ROI-based analysis with seven clusters of significantly lower CMRg in the mild AD dementia group (uncorrected $p \leq 0.005$) but with no difference in CMRa.
Conclusion: Regional brain energy substrate hypometabolism in mild AD dementia may be specific to impaired glucose uptake and/or utilization. This suggests a potential avenue for compensating brain energy deficit in AD dementia with ketones.

Keywords: Acetoacetate, Alzheimer's disease, β-hydroxybutyrate, cerebral metabolic rate, energy metabolism, glucose, ketones

INTRODUCTION

Positron emission tomography (PET) with the glucose tracer, 2-[^{18}F]-fluoro-2-deoxy-D-glucose (^{18}F-FDG), demonstrates that brain glucose uptake is impaired in Alzheimer's disease (AD) at the level of glucose transport and/or phosphorylation by hexokinase [1–3]. The pattern of brain ^{18}F-FDG

*Correspondence to: Christian-Alexandre Castellano, Research Center on Aging, 1036 Belvedere South, Sherbrooke, QC, J1H 4C4, Canada. Tel.: +1 819 780 2220; Fax: +1 819 829 7141; E-mail: Alexandre.Castellano@USherbrooke.ca.

ISSN 1387-2877/15/$27.50

hypometabolism in AD is present initially in the temporoparietal cortex and posterior cingulate, with extension to the frontal cortex as the disease progresses [4]. Lower thalamic ^{18}F-FDG uptake can also be present many years before the onset of clinical symptoms in Presenilin-1 carriers [5]. Suboptimal brain ^{18}F-FDG uptake is also present in individuals at risk of developing AD, i.e., in mild cognitive impairment [6], and in asymptomatic healthy individuals with a maternal family history of AD [7] or carrying the apolipoprotein ε4 allele [8, 9].

The brain's primary fuel is glucose but it also readily uses ketones, particularly during periods of energy deficit and/or hypoglycemia [10–12]. During prolonged fasting, the two ketones, acetoacetate and β-hydroxybutyrate, can supply up to 60% of the human brain's energy requirements [11, 13, 14]. The arteriovenous difference method has shown that in AD brain uptake of ketones may be less disrupted than that of glucose [15, 16]. Lower brain glucose uptake in AD is widely viewed as a consequence of neuronal or synaptic loss and deteriorating brain structure and function. Ketones are transported into brain cells by the monocarboxylic acid transporter, which is distinct from glucose transporters [17, 18]. Ketone entry into the tricarboxylic acid cycle is also independent of glycolysis [10–13]. If brain ketone uptake is not disrupted in AD there are two major implications. First, more neurons may still be functional than previously thought and the brain's metabolic problems could be more-or-less specific to glucose. Hence, at least early in AD, brain dysfunction could be more a function of neuronal exhaustion due to lack of fuel rather than neuronal death. Second, by bypassing defective glucose uptake/utilization to access the tricarboxylic acid cycle and still produce ATP, therapeutic strategies that safely induce mild ketonemia might be able to help rescue neurons before they become too exhausted and thereby potentially delay cognitive deterioration in AD.

The aim of the present study was to determine whether the well-established pattern of lower regional brain FDG hypometabolism in AD is specific to glucose or is also seen with ketones. To address this question, a double tracer PET protocol was used to sequentially assess brain uptake of [^{11}C]-acetoacetate (^{11}C-AcAc) and ^{18}F-FDG in patients with mild AD dementia who were compared with an age-matched group of healthy older adults. This double tracer PET protocol has been used to describe the regional pattern of brain ketone uptake in healthy young and older adults [19] and in rats [20, 21] but not yet in AD.

MATERIALS AND METHODS

Participants

Written informed consent was obtained from all participants prior to enrollment and study approval was granted by the appropriate ethics committees (Health and Social Services Center – Sherbrooke University Geriatrics Institute and the Centre hospitalier universitaire de Sherbrooke). Patients with mild AD dementia ($n = 10$) were identified from newly diagnosed cases at the Memory Disorders Clinic at Health and Social Services Center – Sherbrooke University Geriatrics Institute and referred by a geriatrician or neurologist between January 2010 and September 2012. Participants with mild possible or probable AD dementia were diagnosed according to the National Institute of Neurological and Communicative Disorders and Stroke (NINCDS) and the Alzheimer's Disease and Related Disorders Association (ADRDA) criteria [22]. An age- and gender-matched group of healthy adults (Controls, $n = 29$) were recruited through media advertising. All Controls had a Mini-Mental State Examination (MMSE) score of $\geq$ 27/30 and were taken from a sample of older participants who all had normal cognition [23]. Fasting blood samples were collected for analysis. A medical history questionnaire was also administered. Exclusion criteria included drug addictions, psychiatric diseases, smoking, diabetes, evidence of overt heart, liver or renal disease, and untreated hypertension, dyslipidemia, or thyroid disease. All participants in the mild AD dementia group were taking cholinesterase inhibitors (donepezil, galantamine, or rivastigmine) for at least 3 months prior to study entry. Six of the mild AD dementia patients' were medicated for both hypothyroid disorder (levothyroxine) and dyslipidemia (pravastatin, rosuvastatin, or atorvastatin). Thirteen Controls were taking prescription medication for hypertension (irbesartan, Ramipril, or telmisartan). Five Controls had prescriptions for statins (atorvastatin and rosuvastatin) and five were taking levothyroxine.

Volumetric magnetic resonance (MR) imaging

For each participant, brain MR images were obtained using a 1.5 Tesla scanner (Sonata, Siemens Medical Solutions, Erlangen, Germany). Imaging parameters were - (i) coronal 3D gradient echo acquisition, T1-weight image, TE 4.68 ms, TR 16.0 ms, T1 9.14 min, flip angle 20 degrees, 1 mm^3 isotropic reconstructed voxel size, FOV 256 × 240 × 192 mm^3,

(ii) axial FLAIR image, TE 91 ms, TR 8500 ms, T1 3.09 min, FOV 230×172.5 mm^2; slice thickness of 6 mm.

Regional brain PET

For each participant, brain PET images were obtained on a PET/CT scanner (Gemini TF, Philips Medical System, Eindhoven, The Netherlands). PET images were acquired using a dynamic list mode acquisition, with time-of-flight enabled, an isotropic voxel size of 2 mm^3, field-of-view of 25 cm, and an axial field of 18 cm. Participants fasted for 6–7 h before scanning which started at about 2 pm and was done in a quiet environment with subdued lighting. An indwelling venous catheter was introduced into a forearm vein for blood sampling. A second catheter was placed in the contralateral forearm vein for the injection of the radiotracers. A computed tomography image was obtained for attenuation correction. Each participant was first injected with 5 mCi of ^{11}C-AcAc, due to the shorter 20 min half-life for [^{11}C]. At the end of the ^{11}C-AcAc scan, there was a 50 min rest period for tracer washout. For ^{11}C-AcAc, the time frames were 12×10 s, 8×30 s, and 1×4 min, for a total scan length of 10 min. Participants were subsequently injected with 5 mCi of ^{18}F-FDG. For ^{18}F-FDG, time frames were allocated according to 12×10 s, 8×30 s, 6×4 min, and 3×10 min, for a total scan length of 60 min.

Arterial blood sampling and plasma metabolites

To determine the plasma time–activity curves required for the quantification of brain tracer uptake, blood samples were obtained at 3, 6, and 8 min post ^{11}C-AcAc injection and at 3, 8, 16, 24, 35, and 55 min post ^{18}F-FDG injection. Plasma was separated from red blood cells by centrifugation and 300 μL of plasma was counted in a gamma counter (Cobra, Packard, United States) that was cross-calibrated with the PET scanner. Blood plasma parameters were measured using an automated clinical chemistry analyzer (Dimension Xpand Plus; Siemens Healthcare Diagnostics, Deerfield, IL, USA). Plasma insulin was analyzed by commercial enzyme-linked immunosorbent assay (Alpco, Salem, NH, USA) with a Victor X4 multi-label plate reader (Perkin Elmer, Woodbridge, ON, Canada).

Analysis of PET images

Brain ^{18}F-FDG and ^{11}C-AcAc PET images were analyzed by both region of interest (ROI)- and voxel-based methods. The ROI approach was used to compare uptake of the tracers in specific anatomical regions of the brain whereas the voxel-based approach was used to measure peak differences within a given voxel and permitted easier graphical representation of regions showing hypometabolism. The voxel-based approach is usually considered to be more exploratory than the ROI approach because it does not require the *a priori* selection of specific brain regions. For both methods, brain regional parcellation was based on the Anatomical Automatic Labeling template [24].

Region of interest analysis

All ROI-based analyses were performed using tools implemented in PMOD 3.3 (PMOD Technologies Ltd., Zurich, Switzerland) as previously described by Nugent et al. [19]. Brain PET images for each participant were automatically co-registered to their respective MR images. PET counts were extracted from ROIs defined using the Automated Anatomic Labelling atlas. The modified Müller-Gartner method was applied for partial volume effect (PVE) correction using PMOD 3.3. Arterial input functions were determined by tracing ROIs on the internal carotid arteries with the aid of co-registered MR images as previously validated in humans [25]. The multiple-time graphical analysis technique of Patlak et al. [26] was used to calculate the cerebral metabolic rate (CMR; μmol/100 g/min) of glucose (CMRg) and acetoacetate (CMRa) using the following equation: $CMR = K^*Cp/LC$, where K is the rate constant for net uptake of the tracer, Cp is the arterial plasma concentration of the tracer, and LC is the lumped constant. The *LCs* used for to calculate CMRg and CMRa were set to 0.80 and 1.0, respectively [27, 28]. CMRa was corrected for the loss of 5.9% of the initial injected dose of ^{11}C-AcAc that would have been catabolized to ^{11}C-CO_2 during the ^{11}C-AcAc PET scan [27].

Voxel-based analysis

Using the PMOD 3.3 pixel-wise kinetic modeling tool (PXMOD), parametric images of CMRg and CMRa were produced for each participant. Using SPM8 (Wellcome Trust, London, UK), ^{11}C-AcAc and ^{18}F-FDG images from each participant were normalized to the Montreal Neurological Institute space and corrected for PVE using the modified Müller-Gartner method, which is fully implemented in the PVElab software (http://nru.dk/downloads/software).

Statistical methods

Data are presented as mean ± SD. All statistical analyses were carried out using SPSS 17.0 software (SPSS Inc., Chicago, IL, USA), except for the voxel-based analysis. Grey matter differences between groups for ^{11}C-AcAc and ^{18}F-FDG images were then assessed using a two-sided *t*-test within the general linear model framework of SPM8 software performed in Matlab (MathWorks, Natick, Massachusetts, USA). Dichotomous variables were compared with the Pearson's chi-squared test. Brain regions reported in the tables include only gray matter with white matter being identified separately. Group differences in continuous variables (CMR and *K*) were examined using Mann–Whitney *U*-tests. All ROI-based comparisons underwent a $p \leq 0.05$ false discovery rate (FDR) correction for multiple comparisons. The power to detect a between-group difference of 1.05 SD in mean regional CMR was 79% (nQuery statistical software, Statistical Solutions Ltd., Saugus, MA, USA). Pearson correlation coefficients were used to correlate CMR ROI-based analysis to blood plasma parameters. For the voxel-based analysis, the resulting statistics at each voxel were displayed as SPMs in standard anatomic space, with a minimum cluster size of 100 voxels. An uncorrected $p \leq 0.005$ threshold was used for all voxel-based analysis.

RESULTS

Demographics

Consistent with their diagnosis, the mild AD dementia group had 11% lower scores in global cognition as assessed by the mini mental state examination (MMSE; $p < 0.001$). The two groups did not differ in age, gender ratio, body mass index (BMI), nor any of the blood parameters measured ($p \geq 0.060$; Table 1).

Cerebral metabolic rates of glucose and acetoacetate

Compared to Controls, the mild AD dementia group had 13% lower global CMRg in gray matter as a whole (34.2 ± 5.0 versus 38.5 ± 4.5 μmol/100 g/min, respectively; $p = 0.015$), but no differences in CMRa ($p = 0.412$) or in the rate constants for glucose *(Kg)* or ketones *(Ka)* ($p = 0.105$ and $p = 0.676$, respectively; Fig. 1).

In the ROI-based analysis (Table 2), mild AD dementia patients had 16–33% lower CMRg ($p \leq 0.016$) in the superior, middle, and inferior temporal regions, supramarginal gyrus, precuneus, angular gyrus, cuneus, posterior cingulate, and thalamus (all $p \leq 0.05$ FDR corrected). CMRa did not differ between mild AD dementia patients and Controls in any brain regions ($p \geq 0.188$; Table 3). *Kg* was 19% lower in the precuneus, 30% lower in the angular gyrus, 24% lower in the posterior cingulate, and 16% lower in the thalamus of the mild AD group ($p \leq 0.028$; Table 4). *Ka* did not differ ($p \geq 0.208$) between the two groups in any brain region.

In the voxel-based analysis, the mild AD dementia group had seven clusters of significantly lower CMRg that mainly encompassed the temporal and parietal cortices, as well as subcortical regions including the thalamus ($p \leq 0.005$, Table 5 and Fig. 2). There were no statistically significant clusters for CMRa between the two groups ($p > 0.01$; data not shown).

Plasma ketones and cerebral glucose and ketone uptake

Depending on the brain region, ketone uptake represented 0.7–1.2% of total brain energy consumption, a value that was similar in both groups (data not shown, *all* $p > 0.1$). Plasma acetoacetate was positively correlated to CMRa in both Controls and mild AD dementia ($r = +0.907$ and $r = +0.865$, respectively, *all* $p \leq 0.003$;

Table 1
Characteristics (mean ± SD) of the healthy older persons (Controls, $n = 29$) and patients with mild Alzheimer's disease dementia (Mild AD, $n = 10$)

	Controls	Mild AD	*p*-value
Age (years)	72 ± 5	76 ± 4	0.059
Gender, female (%)	66	60	0.761
MMSE score (30)	29 ± 1	26 ± 2	<0.001*
Weight (kg)	71 ± 16	66 ± 11	0.365
Height (cm)	163 ± 10	167 ± 12	0.475
Body Mass Index	26 ± 4	24 ± 3	0.060
Glucose (mM)	5.2 ± 0.5	5.2 ± 0.6	0.677
Hemoglobin A1c (%)	5.8 ± 0.3	6.0 ± 0.3	0.142
Insulin (IU/L)	5.7 ± 4.1	3.5 ± 2.3	0.084
Acetoacetate (μM)	109 ± 54	106 ± 76	0.759
β-Hydroxybutyrate (μM)	197 ± 112	206 ± 154	0.985
Albumin (g/L)	43 ± 2	44 ± 2	0.239
Cholesterol (mM)	4.6 ± 1.0	4.8 ± 1.5	0.893
HDL cholesterol (mM)	1.5 ± 0.3	1.5 ± 0.4	0.901
LDL cholesterol (mM)	2.8 ± 0.8	2.8 ± 0.8	1.000
Triglycerides (mM)	1.0 ± 0.7	1.0 ± 0.2	0.113
Free fatty acids (mM)	0.9 ± 0.3	1.0 ± 0.4	0.954
Lactate (mM)	1.2 ± 0.4	1.3 ± 0.3	0.397
Creatinine (μmol/L)	71.5 ± 17	81.1 ± 11	0.079
TSH (mIU/L)	2.5 ± 0.8	2.2 ± 1.2	0.222

TSH, thyroid stimulating hormone. *Indicates significance at $p \leq 0.05$.

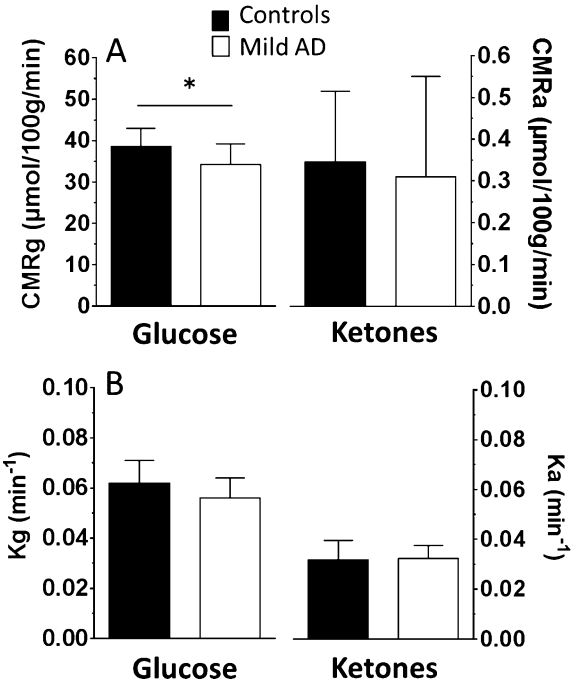

Fig. 1. A) Cerebral metabolic rate of glucose (CMRg; µmol/100 g/min) and acetoacetate (CMRa; µmol/100 g/min) and (B) mean rate constant for glucose (*Kg*; min^{-1}) and acetoacetate (*Ka*; min^{-1}) for global gray matter in healthy older persons (Controls) and mild Alzheimer's disease dementia (Mild AD). All values are mean ± SD. $^{*}p < 0.05$ after correction for multiple comparisons. The mild AD dementia group had a lower global CMRg (−13%; $p = 0.015$) but no difference in CMRa ($p = 0.412$) compared to Controls. There was no difference for *Kg* or *Ka* between the two groups ($p = 0.105$ and $p = 0.676$, respectively).

Fig. 3A), with no statistically significant difference between the two correlations ($z = 0.463$, $p = 0.640$). CMRg and CMRa were negatively correlated in the mild AD dementia group ($r = -0.922$, $p \leq 0.001$) but not in the Controls ($r = -0.060$, $p = 0.762$; Fig. 3B).

DISCUSSION

To the best of our knowledge, this is the first quantitative, PET-based assessment of regional brain glucose and ketone metabolism in mild AD dementia. Our main observation is that in comparison with cognitively healthy age-matched older persons, the well-known regional deficit in brain glucose uptake in mild AD dementia was not observed for brain ketone uptake. Our PET ^{18}F-FDG findings agree with previous reports showing characteristic temporoparietal hypometabolism for glucose in the early stages of AD [29–34]. Thus, in mild AD dementia, brain regions with a decreased ability to acquire and/or consume glucose still appear able to take up and use ketones normally. This suggests that brain glucose hypometabolism in mild AD dementia is not necessarily a reflection of a generalized problem with brain fuel uptake but may be specific to glucose.

Table 2
Cerebral metabolic rate of glucose (µmol/100 g/min; mean ± SD) in healthy older persons (Controls, $n = 29$) and mild Alzheimer's disease dementia (Mild AD, $n = 10$)

Brain regions	Controls	Mild AD	*p-value*
Frontal cortex			
Frontal superior	41.2 ± 7.4	37.5 ± 6.0	0.145
Frontal medial	43.1 ± 6.6	37.9 ± 6.3	0.031
Frontal inferior	42.2 ± 4.1	38.3 ± 6.1	0.105
Precentral gyrus	50.4 ± 6.9	48.3 ± 7.4	0.558
Rectus	33.8 ± 5.2	32.3 ± 4.5	0.716
Supplementary motor	46.2 ± 7.5	43.6 ± 6.8	0.437
Temporal cortex			
Superior/middle/inferior	33.6 ± 5.8	29.0 ± 5.6	0.013*
Para/hippocampus	23.3 ± 3.0	21.7 ± 3.8	0.219
Fusiform	30.0 ± 3.4	27.9 ± 5.1	0.185
Parietal cortex			
Superior/inferior	48.3 ± 7.6	41.2 ± 9.7	0.079
Supramarginal gyrus	41.1 ± 5.0	34.6 ± 6.8	0.011*
Postcentral gyrus	52.4 ± 7.2	50.9 ± 7.7	0.678
Precuneus	43.0 ± 6.0	35.7 ± 5.5	0.002*
Angular gyrus	45.7 ± 6.9	34.5 ± 8.4	0.001*
Occipital cortex			
Calcarine	42.6 ± 6.4	39.1 ± 6.1	0.145
Cuneus	49.2 ± 7.8	41.8 ± 6.7	0.016*
Lingual	37.7 ± 5.5	36.1 ± 6.2	0.669
Cingulate cortex			
Anterior	29.9 ± 5.1	27.7 ± 4.8	0.185
Middle	39.6 ± 5.0	37.2 ± 5.2	0.185
Posterior	47.6 ± 8.5	37.7 ± 6.3	0.002*
Rolandic operculum	35.5 ± 4.8	32.8 ± 4.0	0.246
Amygdala	19.3 ± 3.2	17.4 ± 2.4	0.136
Insula	32.6 ± 3.6	31.7 ± 4.5	0.558
Caudate	35.7 ± 7.1	31.6 ± 5.8	0.069
Putamen	42.9 ± 5.6	39.6 ± 6.3	0.185
Thalamus	36.4 ± 5.8	31.0 ± 7.1	0.011*
Cerebellum	25.9 ± 4.0	25.4 ± 4.2	0.962
White matter	15.4 ± 1.8	14.0 ± 2.3	0.164

*Statistically significant difference between the Control and Mild AD groups after $p \leq 0.05$ false discovery rate correction for multiple comparisons.

Because of the logistical constraints associated with a dynamic PET acquisitions, few ^{18}F-FDG PET studies now report regional brain *Kg* in AD [29, 35, 36]. Our results support the suggestion by Mosconi and colleagues [36], that lower *Kg* closely mimics neuropathological changes observed during the progression of AD. Irrespective of whether the data were expressed as *Ka* or CMRa, or whether the analysis was ROI- or voxel-based, there were no differences in brain ketone uptake between the two groups. Therefore, we confirm previous A-V difference studies demonstrating no statistically significant difference in brain

Table 3
Cerebral metabolic rate of acetoacetate (μmol/100 g/min; mean ± SD) in healthy older persons (Controls, $n = 28$) and in mild Alzheimer's disease dementia (Mild AD, $n = 9$)

Brain regions	Controls	Mild AD	p-value
Frontal cortex			
Frontal superior	0.33 ± 0.19	0.30 ± 0.25	0.412
Frontal medial	0.35 ± 0.19	0.31 ± 0.25	0.302
Frontal inferior	0.35 ± 0.19	0.31 ± 0.26	0.319
Precentral gyrus	0.39 ± 0.20	0.35 ± 0.29	0.355
Rectus	0.30 ± 0.19	0.25 ± 0.20	0.286
Supplementary motor	0.40 ± 0.22	0.33 ± 0.26	0.188
Temporal cortex			
Superior/middle/inferior	0.34 ± 0.17	0.32 ± 0.25	0.542
Para/hipoccampus	0.27 ± 0.14	0.26 ± 0.22	0.433
Fusiform	0.33 ± 0.17	0.30 ± 0.24	0.475
Parietal cortex			
Superior/inferior	0.40 ± 0.21	0.36 ± 0.29	0.433
Supramarginal gyrus	0.37 ± 0.18	0.33 ± 0.26	0.355
Postcentral gyrus	0.41 ± 0.23	0.38 ± 0.30	0.412
Precuneus	0.41 ± 0.20	0.37 ± 0.29	0.412
Angular gyrus	0.41 ± 0.21	0.37 ± 0.30	0.453
Occipital cortex			
Calcarine	0.42 ± 0.21	0.37 ± 0.28	0.379
Cuneus	0.49 ± 0.26	0.42 ± 0.31	0.392
Lingual	0.40 ± 0.20	0.35 ± 0.25	0.519
Cingulate cortex			
Anterior	0.27 ± 0.14	0.24 ± 0.20	0.240
Middle	0.35 ± 0.17	0.32 ± 0.27	0.319
Posterior	0.38 ± 0.21	0.40 ± 0.28	0.958
Rolandic operculum	0.29 ± 0.16	0.26 ± 0.22	0.355
Amygdala	0.23 ± 0.14	0.19 ± 0.14	0.433
Insula	0.28 ± 0.15	0.26 ± 0.22	0.542
Caudate	0.21 ± 0.13	0.17 ± 0.15	0.240
Putamen	0.33 ± 0.19	0.29 ± 0.26	0.336
Thalamus	0.34 ± 0.19	0.28 ± 0.20	0.302
Cerebellum	0.29 ± 0.16	0.27 ± 0.23	0.453
White matter	0.16 ± 0.08	0.15 ± 0.12	0.336

Table 4
Rate constant for glucose (Kg; $min^{-1} \times 10^{-2}$) and acetoacetate (Ka; $min^{-1} \times 10^{-2}$; both mean ± SD) in healthy older persons (Controls, $n = 28$) and mild Alzheimer's disease dementia (Mild AD, $n = 9$)

Brain regions	*Kg*		*Ka*	
	Controls	Mild AD	Controls	Mild AD
Frontal cortex				
Frontal superior	6.7 ± 1.3	6.2 ± 0.9	3.0 ± 1.0	3.1 ± 0.6
Frontal medial	7.0 ± 1.2	6.2 ± 1.0	3.1 ± 0.9	3.1 ± 0.6
Frontal inferior	6.8 ± 1.0	6.3 ± 1.0	3.1 ± 0.8	3.2 ± 0.6
Precentral gyrus	8.1 ± 1.4	7.9 ± 1.2	3.5 ± 0.8	3.5 ± 0.5
Rectus	5.4 ± 0.9	5.3 ± 0.9	2.7 ± 1.1	2.7 ± 0.7
Supplementary motor	7.5 ± 1.3	7.1 ± 0.9	3.6 ± 1.0	3.5 ± 1.1
Temporal cortex				
Superior/middle/ inferior	5.4 ± 0.8	4.8 ± 0.9	3.1 ± 0.8	3.3 ± 0.7
Para/hippocampus	3.8 ± 0.6	3.6 ± 0.6	2.5 ± 0.6	2.6 ± 0.6
Fusiform	4.8 ± 0.7	4.6 ± 0.9	3.0 ± 0.8	3.1 ± 0.5
Parietal cortex				
Superior/inferior	7.8 ± 1.4	6.7 ± 1.5	3.7 ± 1.1	3.6 ± 0.6
Supramarginal gyrus	6.6 ± 1.0	5.7 ± 1.1	3.3 ± 0.8	3.4 ± 0.6
Postcentral gyrus	8.5 ± 1.4	8.3 ± 1.1	3.7 ± 1.2	3.8 ± 0.6
Precuneus	6.9 ± 1.1	5.9 ± 0.9*	3.7 ± 1.0	3.8 ± 0.6
Angular gyrus	7.4 ± 1.3	5.7 ± 1.5*	3.7 ± 0.9	3.8 ± 0.7
Occipital cortex				
Calcarine	6.9 ± 1.2	6.4 ± 1.0	3.8 ± 1.0	3.9 ± 0.7
Cuneus	7.9 ± 1.4	6.9 ± 1.1*	4.4 ± 1.1	4.5 ± 0.9
Lingual	6.1 ± 1.0	5.9 ± 0.9	3.6 ± 0.9	3.8 ± 0.7
Cingulate cortex				
Anterior	4.8 ± 0.9	4.5 ± 0.6	2.5 ± 0.6	2.4 ± 0.7
Middle	6.4 ± 1.0	6.1 ± 0.8	3.2 ± 0.8	3.3 ± 0.7
Posterior	7.6 ± 1.5	6.2 ± 1.1*	3.5 ± 1.3	4.2 ± 1.1
Rolandic operculum	5.7 ± 0.9	5.4 ± 0.6	2.6 ± 0.9	2.6 ± 0.5
Amygdala	3.1 ± 0.6	2.9 ± 0.4	2.1 ± 0.9	2.0 ± 0.7
Insula	5.2 ± 0.01	5.2 ± 0.7	2.5 ± 0.7	2.6 ± 0.4
Caudate	5.7 ± 1.2	5.2 ± 0.7	1.9 ± 0.6	1.5 ± 0.9
Putamen	6.9 ± 1.0	6.5 ± 1.1	2.9 ± 0.9	2.8 ± 0.7
Thalamus	5.9 ± 1.0	5.1 ± 1.0*	3.0 ± 1.0	2.9 ± 0.8
Cerebellum	4.2 ± 0.7	4.2 ± 0.8	2.6 ± 0.7	2.8 ± 0.6
White matter	2.5 ± 0.4	2.3 ± 0.4	1.4 ± 0.4	1.5 ± 0.3

*Statistically significant difference between the Control and Mild AD groups after $P \leq 0.05$ false discovery rate correction for multiple comparisons.

ketone metabolism in AD [15, 16] and show that this observation remains true not only for the brain as a whole but also at the regional level. Brain ketone uptake has repeatedly been shown to be linear and to vary directly with plasma ketone concentrations over at least a 400 fold range (20 μM–8 mM) [14, 19, 27, 37, 38]. In the present study, there were no significant differences in plasma ketone concentrations between the two groups at the time of the PET scans, nor in the slope of the linear relationship between plasma acetoacetate concentrations and brain ^{11}C-AcAc uptake (Fig. 3A).

There was a negative correlation between CMRg and CMRa in mild AD dementia that was not present in the Controls (Fig. 3B). It is therefore possible that brain regions with the most severe glucose hypometabolism in mild AD dementia may be able to switch to some extent to ketone metabolism, an interpretation supported by the significant inverse correlation between CMRg and CMRa uptake in the mild AD dementia group. The patients with mild AD dementia who exhibited the lowest global CMRg (25.1 ± 6.9 μmol/100 g/min, which is 32% below the mean uptake of age-matched normal controls), had a CMRa of 0.8 μmol/100 g/min (Fig. 3B). Hence, under our study conditions, higher CMRa did not fully compensate for a deficit in CMRg in the mild AD dementia group. As previously reported in a transgenic mouse model of AD [39], plasma β-hydroxybutyrate commonly reaches 0.5 mM in humans in nutritional ketosis, a level that theoretically could largely compensate for the deficit in brain glucose uptake [10]. Our dual tracer PET protocol can be applied to assessing whether there are changes in brain energy substrate metabolism in older adults with mild cognitive impairment or AD

Table 5
Seven clusters with significantly lower cerebral metabolic rate of glucose from voxel-based analysis were observed in mild Alzheimer's disease dementia

Coordinates (mm)*			Anatomical regions	% Cluster	Nb Vx cluster	% Label	Cluster size
x	y	z					
51	−67	28	Right superior temporal	47.5	564	1.1	3141
			Right inferior parietal	22.7	564	1.2	1345
			Right angular gyrus	4.3	564	0.2	1752
			Right middle temporal	1.4	564	0.1	4409
			Right middle occipital	0.2	564	0.1	2098
4	−16	2	Right thalamus	3.8	787	0.3	1057
−10	−24	8	Left thalamus	0.9	756	0.1	1100
			Left hippocampus	0.8	756	0.1	932
−15	6	14	Left caudate	4.9	304	0.2	962
−61	−46	−19	Left inferior temporal	28.4	408	0.4	3200
			Left middle temporal	5.4	408	0.1	4942
15	−1	14	Right caudate	1.5	324	0.1	994
−4	−58	26	Left precuneus	4.1	122	0.1	3528
			Left cuneus	2.5	122	0.1	1526
			Left posterior cingulum	0.8	122	0.1	463

*Coordinates in MNI space. % Cluster: percent of cluster volume included within labeled region. Nb Vx cluster: number of voxels in cluster. % Label: percent of label encompassed by cluster. Cluster size in voxels, voxel size = 1 × 1 × 1 mm. Cluster size threshold was 100 voxels, uncorrected $p \leq 0.005$ threshold.

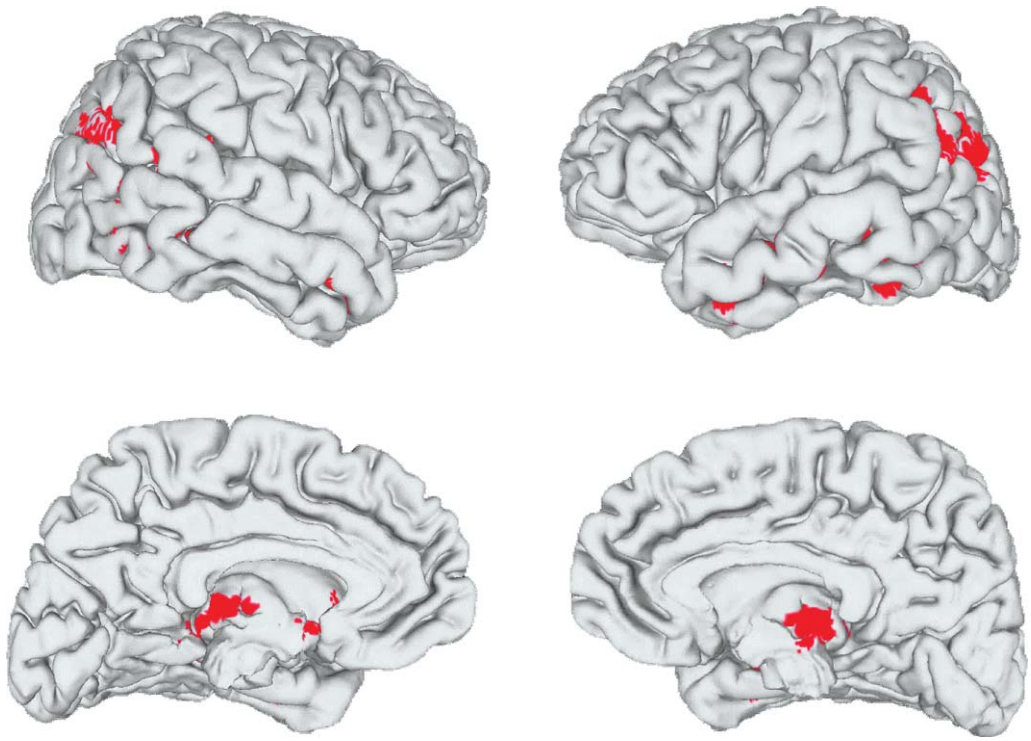

Fig. 2. Brain areas in red had lower regional cerebral metabolic rate of glucose (μmol/100 g/min) in mild Alzheimer's disease dementia (Mild AD) compared to healthy older persons (Controls). The images were smoothed by a Gaussian kernel with a full width at half maximum of 8 mm. For purposes of illustration, voxel-wise statistics surviving $p < 0.05$ are displayed. The mild AD dementia group had seven clusters of significantly lower CMRg that encompassed mainly the temporal and parietal cortex and thalamus.

who are receiving dietary ketogenic interventions in an attempt to improve cognitive outcomes [40–42]. Older persons consuming a ketogenic diet over two to twelve months experience improved cognitive performance, particularly working memory and processing speed [43, 44]. Following a 3-week ketogenic diet,

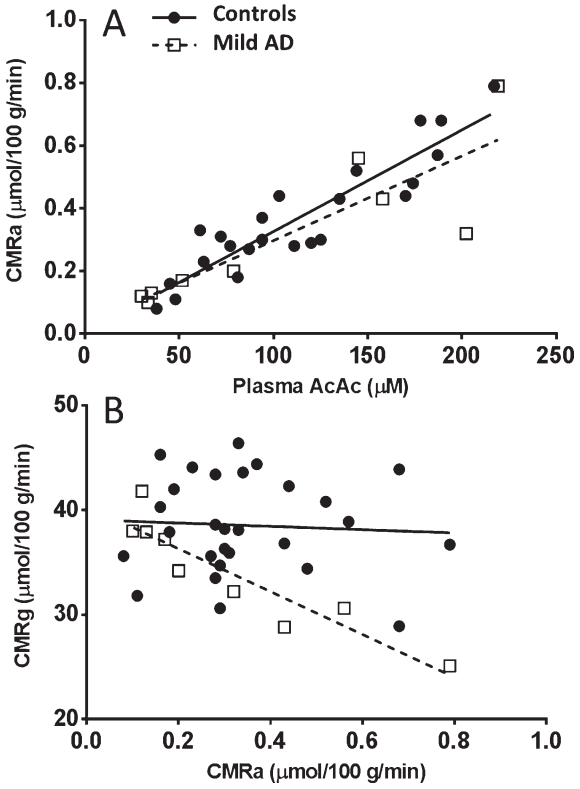

Fig. 3. A) Cerebral metabolic rate of acetoacetate (CMRa) plotted against fasting plasma acetoacetate (AcAc). Each point represents mean global brain CMRa for a single participant. Plasma AcAc and CMRa were significantly positively correlated in both the cognitively healthy older group (Controls; $r = +0.907$, $p \leq 0.001$) and in mild Alzheimer's disease dementia (Mild AD; $r = +0.865$, $p = 0.003$). There was no significant difference between the two correlation coefficients ($z = 0.463$, $p = 0.640$). B) Cerebral metabolic rate of glucose (CMRg) plotted against cerebral metabolic rate of acetoacetate (CMRa). Each point represents the global mean brain CMR value for a single participant. CMRg and CMRa were significantly negatively correlated in the mild Alzheimer's disease dementia group (Mild AD; $r = -0.922$, $p \leq 0.001$) but not in healthy older group (Controls; $r = -0.060$, $p = 0.762$).

blood ketones can increase to 0.5 mM in non-diabetic persons [45] and 2–3 mM in non-insulin dependent diabetics [46], an amount that could support 10–30% of total brain energy metabolism [10, 38].

Our dynamic PET results revealed 22% lower CMRg in the parietal and temporal cortices of the mild AD dementia patients compared to the Controls. We have previously reported that global brain glucose uptake is 8% lower in healthy older persons than in young adults [19]. The 8% value masks somewhat the more important deficit in CMRg localized principally in the frontal cortex (−15%) and some subcortical nuclei (−14%). Glucose hypometabolism in AD is reported in regions that are generally not affected during the normal aging process [47]. However, Dukart and colleagues recently showed an overlap in the pattern of regional brain glucose hypometabolism in healthy aging and in AD, suggesting regional similarity between AD pathology and aging-related processes [48].

We have previously reported that raising plasma ketones with a ketogenic diet in rats not only increases brain ketone uptake but also increases brain ^{18}F-FDG uptake [20, 21]. Ketones also reportedly improve mitochondrial ATP production and synaptic function in an *ex vivo* rat hippocampal preparation [49]. Taken together, these results suggest that increasing energy availability to glucose-deficient brain regions by increasing glucose (^{18}F-FDG) uptake or by providing alternative energy substrates such as ketones is a potential complementary strategy for the treatment of early AD.

The present study extends previous research by using an age- and gender-matched design to optimize ^{18}F-FDG PET [50]. The two tracers were injected sequentially during the same afternoon to minimize biological variability and improve comparability between the two brain fuels. PVE correction was also applied to the PET images to yield a more accurate quantification of cerebral glucose/ketone uptake. Nevertheless, this study has several limitations, including the unknown extent to which CMRa is sensitive to brain changes occurring in moderate to severe AD dementia. There was also a small number of patients in the mild AD dementia group. The mild AD dementia patients were all treated with an anticholinesterase, which could potentially have improved brain metabolic activity [51–53]. Both groups included participants who were on medications for hypertension, hypercholesterolemia, or thyroid replacement but, in our experience, these medications do not affect brain glucose uptake [23]. PET provides relatively low image resolution that cannot distinguish between neurons, astrocytes, and oligodendrocytes. Without higher resolution, the brain cell types that are less able to acquire or use glucose but still use ketones remains open to speculation. Whether the brain cells that have abnormal glucose transporters [54], neuronal mitochondrial dysfunction [55], or different energy substrate preference (glucose in neurons versus ketones in astrocytes) [56] are the same as those that can still use ketones is also unknown. All participants were fasted for 6–7 hours which induces a degree of mild ketosis that varies significantly between individuals, making brain ketone uptake values more variable than for glucose. Under the conditions of the present

study, plasma ketones contributed about 1% of total brain energy metabolism. Raising plasma ketones was not an objective of this study, but it would be useful to assess brain ^{18}F-FDG and ^{11}C-AcAc uptake during nutritional ketosis in which plasma ketones are somewhat closer to the postulated therapeutic concentration of 0.5 mM [10, 38, 57].

We conclude that lower regional brain glucose (^{18}F-FDG) uptake in mild AD dementia is not observed for ^{11}C-AcAc under conditions in which plasma ketones are relatively low. The reported therapeutic benefits of mild nutritional ketosis for cognition in mild AD or mild cognitive impairment may be partly linked to the less impeded uptake of this key alternative brain fuel.

ACKNOWLEDGMENTS

Travel expenses to attend conferences have been provided to CAC by Accera Ltd (Broomfield, CO, USA). Financial support for the research described herein came from government sources including the Canada Research Chairs secretariat, CIHR, NSERC, CFI, Université de Sherbrooke (Faculty of Medicine and Health Sciences and the Department of Medicine), the Sherbrooke Molecular Imaging Center, the CHUS Research Centre, and the Research Center on Aging (both FRSQ funded), and FQRNT (CFQCU program). Excellent assistance was provided by Mélanie Fortier, Conrad Filteau, Esteban Espinosa and Éric Lavallée.

Authors' disclosures available online (http://www.j-alz.com/disclosures/view.php?id=2475).

REFERENCES

[1] Dehghan H, Pouyan AA, Hassanpour H (2014) Detection of Alzheimer's disease using multitracer positron emission tomography imaging. *Int J Eng* **27**, 51-56.

[2] Piert M, Koeppe RA, Giordani B, Berent S, Kuhl DE (1996) Diminished glucose transport and phosphorylation in Alzheimer's disease determined by dynamic FDG-PET. *J Nucl Med* **37**, 201-208.

[3] Marcus DL, Freedman ML (1997) Decreased brain glucose metabolism in microvessels from patients with Alzheimer's disease. *Ann N Y Acad Sci* **826**, 248-253.

[4] Nordberg A, Rinne JO, Kadir A, Långström B (2010) The use of PET in Alzheimer disease. *Nat Rev Neurol* **6**, 78-87.

[5] Scholl M, Almkvist O, Axelman K, Stefanova E, Wall A, Westman E, Langstrom B, Lannfelt L, Graff C, Nordberg A (2011) Glucose metabolism and PIB binding in carriers of a His163Tyr presenilin 1 mutation. *Neurobiol Aging* **32**, 1388-1399.

[6] Mosconi L, Andrews RD, Matthews DC (2013) Comparing brain amyloid deposition, glucose metabolism, and atrophy in mild cognitive impairment with and without a family history of dementia. *J Alzheimers Dis* **35**, 509-524.

[7] Mosconi L, Brys M, Switalski R, Mistur R, Glodzik L, Pirraglia E, Tsui W, De Santi S, De Leon MJ (2007) Maternal family history of Alzheimer's disease predisposes to reduced brain glucose metabolism. *Proc Natl Acad Sci U S A* **104**, 19067-19072.

[8] Reiman EM, Chen K, Alexander GE, Caselli RJ, Bandy D, Osborne D, Saunders AM, Hardy J (2005) Correlations between apolipoprotein E epsilon4 gene dose and brain-imaging measurements of regional hypometabolism. *Proc Natl Acad Sci U S A* **102**, 8299-8302.

[9] Langbaum JB, Chen K, Caselli RJ, Lee W, Reschke C, Bandy D, Alexander GE, Burns CM, Kaszniak AW, Reeder SA, Corneveaux JJ, Allen AN, Pruzin J, Huentelman MJ, Fleisher AS, Reiman EM (2010) Hypometabolism in Alzheimer-affected brain regions in cognitively healthy Latino individuals carrying the apolipoprotein E epsilon4 allele. *Arch Neurol* **67**, 462-468.

[10] Cunnane S, Nugent S, Roy M, Courchesne-Loyer A, Croteau E, Tremblay S, Castellano A, Pifferi F, Bocti C, Paquet N, Begdouri H, Bentourkia M, Turcotte E, Allard M, Barberger-Gateau P, Fulop T, Rapoport SI (2011) Brain fuel metabolism, aging, and Alzheimer's disease. *Nutrition* **27**, 3-20.

[11] Cahill GF (2006) Fuel metabolism in starvation. *Annu Rev Nutr* **26**, 1-22.

[12] Mamelak M (2012) Sporadic Alzheimer's disease: The starving brain. *J Alzheimers Dis* **31**, 459-474.

[13] Veech RL, Chance B, Kashiwaya Y, Lardy HA, Cahill GF Jr (2001) Ketone bodies, potential therapeutic uses. *IUBMB Life* **51**, 241-247.

[14] Owen OE, Morgan AP, Kemp HG, Sullivan JM, Herrera MG, Cahill GF Jr (1967) Brain metabolism during fasting. *J Clin Invest* **46**, 1589-1595.

[15] Ogawa M, Fukuyama H, Ouchi Y, Yamauchi H, Kimura J (1996) Altered energy metabolism in Alzheimer's disease. *J Neurol Sci* **139**, 78-82.

[16] Lying-Tunell U, Lindblad BS, Malmlund HO, Persson B (1981) Cerebral blood flow and metabolic rate of oxygen, glucose, lactate, pyruvate, ketone bodies and amino acids. II. Presenile dementia and normal-pressure hydrocephalus. *Acta Neurol Scand* **63**, 337-350.

[17] Simpson IA, Carruthers A, Vannucci SJ (2007) Supply and demand in cerebral energy metabolism: The role of nutrient transporters. *J Cereb Blood Flow Metab* **27**, 1766-1791.

[18] Halestrap AP (2013) Monocarboxylic acid transport. *Compr Physiol* **3**, 1611-1643.

[19] Nugent S, Tremblay S, Chen KW, Ayutyanont N, Roontiva A, Castellano CA, Fortier M, Roy M, Courchesne-Loyer A, Bocti C, Lepage M, Turcotte E, Fulop T, Reiman EM, Cunnane SC (2014) Brain glucose and acetoacetate metabolism: A comparison of young and older adults. *Neurobiol Aging* **35**, 1386-1395.

[20] Pifferi F, Tremblay S, Croteau E, Fortier M, Tremblay-Mercier J, Lecomte R, Cunnane SC (2011) Mild experimental ketosis increases brain uptake of 11C-acetoacetate and 18 F-fluorodeoxyglucose: A dual-tracer pet imaging study in rats. *Nutr Neurosci* **14**, 51-58.

[21] Roy M, Nugent S, Tremblay-Mercier J, Tremblay S, Courchesne-Loyer A, Beaudoin JF, Tremblay L, Descoteaux M, Lecomte R, Cunnane SC (2012) The ketogenic diet increases brain glucose and ketone uptake in aged rats: A dual tracer PET and volumetric MRI study. *Brain Res* **1488**, 14-23.

[22] McKhann GM, Knopman DS, Chertkow H, Hyman BT, Jack CR Jr, Kawas CH, Klunk WE, Koroshetz WJ, Manly JJ, Mayeux R, Mohs RC, Morris JC, Rossor MN,

Scheltens P, Carrillo MC, Thies B, Weintraub S, Phelps CH (2011) The diagnosis of dementia due to Alzheimer's disease: Recommendations from the National Institute on Aging-Alzheimer's Association workgroups on diagnostic guidelines for Alzheimer's disease. *Alzheimers Dement* **7**, 263-269.

[23] Nugent S, Castellano C, Goffaux P, Whittingstall K, Lepage M, Paquet N, Bocti C, Fulop T, Cunnane S (2014) Glucose hypometabolism is highly localized but lower cortical thickness and brain atrophy are widespread in cognitively normal older adults. *Am J Physiol Endocrinol Metab* **306**, E1315-E1321.

[24] Tzourio-Mazoyer N, Landeau B, Papathanassiou D, Crivello F, Etard O, Delcroix N, Mazoyer B, Joliot M (2002) Automated anatomical labeling of activations in SPM using a macroscopic anatomical parcellation of the MNI MRI single-subject brain. *Neuroimage* **15**, 273-289.

[25] Zhou L, Wang Y, Li Y, Yap PT, Shen D (2011) Hierarchical anatomical brain networks for MCI prediction: Revisiting volumetric measures. *PloS One* **6**, e21935.

[26] Patlak CS, Blasberg RG, Fenstermacher JD (1983) Graphical evaluation of blood-to-brain transfer constants from multiple-time uptake data. *J Cereb Blood Flow Metab* **3**, 1-7.

[27] Blomqvist G, Thorell JO, Ingvar M, Grill V, Widen L, Stone-Elander S (1995) Use of R-beta-[1-11C]hydroxybutyrate in PET studies of regional cerebral uptake of ketone bodies in humans. *Am J Physiol* **269**, E948-E959.

[28] Graham MM, Muzi M, Spence AM, O'Sullivan F, Lewellen TK, Link JM, Krohn KA (2002) The FDG lumped constant in normal human brain. *J Nucl Med* **43**, 1157-1166.

[29] Friedland RP, Jagust WJ, Huesman RH, Koss E, Knittel B, Mathis CA, Ober BA, Mazoyer BM, Budinger TF (1989) Regional cerebral glucose transport and utilization in Alzheimer's disease. *Neurology* **39**, 1427-1434.

[30] Ibanez V, Pietrini P, Alexander GE, Furey ML, Teichberg D, Rajapakse JC, Rapoport SI, Schapiro MB, Horwitz B (1998) Regional glucose metabolic abnormalities are not the result of atrophy in Alzheimer's disease. *Neurology* **50**, 1585-1593.

[31] Duara R, Grady C, Haxby J, Sundaram M, Cutler NR, Heston L, Moore A, Schlageter N, Larson S, Rapoport SI (1986) Positron emission tomography in Alzheimer's disease. *Neurology* **36**, 879-887.

[32] Hoffman JM, Welsh-Bohmer KA, Hanson M, Crain B, Hulette C, Earl N, Coleman RE (2000) FDG PET imaging in patients with pathologically verified dementia. *J Nucl Med* **41**, 1920-1928.

[33] Mosconi L (2005) Brain glucose metabolism in the early and specific diagnosis of Alzheimer's disease: FDG-PET studies in MCI and AD. *Eur J Nucl Med Mol Imaging* **32**, 486-510.

[34] Bokde ALW, Teipel SJ, Drzezga A, Thissen J, Bartenstein P, Dong W, Leinsinger G, Born C, Schwaiger M, Moeller HJ, Hampel H (2005) Association between cognitive performance and cortical glucose metabolism in patients with mild Alzheimer's disease. *Dement Geriatr Cogn Disord* **20**, 352-357.

[35] Jagust WJ, Seab JP, Huesman RH, Valk PE, Mathis CA, Reed BR, Coxson PG, Budinger TF (1991) Diminished glucose transport in alzheimer's disease: Dynamic PET studies. *J Cereb Blood Flow Metab* **11**, 323-330.

[36] Mosconi L, Tsui WH, Rusinek H, De Santi S, Li Y, Wang GJ, Pupi A, Fowler J, de Leon MJ (2007) Quantitation, regional vulnerability, and kinetic modeling of brain glucose metabolism in mild Alzheimer's disease. *Eur J Nucl Med Mol Imaging* **34**, 1467-1479.

[37] Hasselbalch SG, Knudsen GM, Jakobsen J, Hageman LP, Holm S, Paulson OB (1995) Blood-brain barrier permeability of glucose and ketone bodies during short-term starvation in humans. *Am J Physiol* **268**, E1161-E1166.

[38] Courchesne-Loyer A, Fortier M, Tremblay-Mercier J, Chouinard-Watkins R, Roy M, Nugent S, Castellano CA, Cunnane SC (2013) Stimulation of mild, sustained ketonemia by medium-chain triacylglycerols in healthy humans: Estimated potential contribution to brain energy metabolism. *Nutrition* **29**, 635-640.

[39] Yao J, Irwin RW, Zhao L, Nilsen J, Hamilton RT, Brinton RD (2009) Mitochondrial bioenergetic deficit precedes Alzheimer's pathology in female mouse model of Alzheimer's disease. *Proc Natl Acad Sci U S A* **106**, 14670-14675.

[40] Krikorian R, Shidler MD, Dangelo K, Couch SC, Benoit SC, Clegg DJ (2012) Dietary ketosis enhances memory in mild cognitive impairment. *Neurobiol Aging* **33**, 425 e419-e427.

[41] Reger MA, Henderson ST, Hale C, Cholerton B, Baker LD, Watson GS, Hyde K, Chapman D, Craft S (2004) Effects of β-hydroxybutyrate on cognition in memory-impaired adults. *Neurobiol Aging* **25**, 311-314.

[42] Henderson ST, Vogel JL, Barr LJ, Garvin F, Jones JJ, Costantini LC (2009) Study of the ketogenic agent AC-1202 in mild to moderate Alzheimer's disease: A randomized, double-blind, placebo-controlled, multicenter trial. *Nutr Metab (Lond)* **6**, 31.

[43] Halyburton AK, Brinkworth GD, Wilson CJ, Noakes M, Buckley JD, Keogh JB, Clifton PM (2007) Low- and high-carbohydrate weight-loss diets have similar effects on mood but not cognitive performance. *Am J Clin Nutr* **86**, 580-587.

[44] Brinkworth GD, Buckley JD, Noakes M, Clifton PM, Wilson CJ (2009) Long-term effects of a very low-carbohydrate diet and a low-fat diet on mood and cognitive function. *Arch Intern Med* **169**, 1873-1880.

[45] Noakes M, Foster PR, Keogh JB, James AP, Mamo JC, Clifton PM (2006) Comparison of isocaloric very low carbohydrate/high saturated fat and high carbohydrate/low saturated fat diets on body composition and cardiovascular risk. *Nutr Metab (Lond)* **3**, 7.

[46] Gumbiner B, Wendel JA, McDermott MP (1996) Effects of diet composition and ketosis on glycemia during very-low-energy-diet therapy in obese patients with non-insulin-dependent diabetes mellitus. *Am J Clin Nutr* **63**, 110-115.

[47] Herholz K, Salmon E, Perani D, Baron JC, Holthoff V, Frölich L, Schönknecht P, Ito K, Mielke R, Kalbe E, Zündorf G, Delbeuck X, Pelati O, Anchisi D, Fazio F, Kerrouche N, Desgranges B, Eustache F, Beuthien-Baumann B, Menzel C, Schröder J, Kato T, Arahata Y, Henze M, Heiss WD (2002) Discrimination between Alzheimer dementia and controls by automated analysis of multicenter FDG PET. *Neuroimage* **17**, 302-316.

[48] Dukart J, Kherif F, Mueller K, Adaszewski S, Schroeter ML, Frackowiak RSJ, Draganski B (2013) Generative FDG-PET and MRI model of aging and disease progression in Alzheimer's disease. *PLoS Comput Biol* **9**, e1002987.

[49] Kim DY, Vallejo J, Rho JM (2010) Ketones prevent synaptic dysfunction induced by mitochondrial respiratory complex inhibitors. *J Neurochem* **114**, 130-141.

[50] Willis MW, Ketter TA, Kimbrell TA, George MS, Herscovitch P, Danielson AL, Benson BE, Post RM (2002) Age, sex and laterality effects on cerebral glucose metabolism in healthy adults. *Psychiatry Res* **114**, 23-37.

[51] Shimada A, Hashimoto H, Kawabe J, Higashiyama S, Kai T, Kataoka K, Tagawa R, Kawarada Y, Nakanishi A, Inoue K,

Shiomi S, Kiriike N (2011) Evaluation of therapeutic response to donepezil by positron emission tomography. *Osaka City Med J* **57**, 11-19.

[52] Potkin SG, Anand R, Fleming K, Alva G, Keator D, Carreon D, Messina J, Wu JC, Hartman R, Fallon JH (2001) Brain metabolic and clinical effects of rivastigmine in Alzheimer's disease. *Int J Neuropsychopharmacol* **4**, 223-230.

[53] Keller C, Kadir A, Forsberg A, Porras O, Nordberg A (2011) Long-term effects of galantamine treatment on brain functional activities as measured by PET in Alzheimer's disease patients. *J Alzheimers Dis* **24**, 109-123.

[54] Liu Y, Liu F, Iqbal K, Grundke-Iqbal I, Gong CX (2008) Decreased glucose transporters correlate to abnormal hyperphosphorylation of tau in Alzheimer disease. *FEBS Lett* **582**, 359-364.

[55] Hirai K, Aliev G, Nunomura A, Fujioka H, Russell RL, Atwood CS, Johnson AB, Kress Y, Vinters HV, Tabaton M, Shimohama S, Cash AD, Siedlak SL, Harris PLR, Jones PK, Petersen RB, Perry G, Smith MA (2001) Mitochondrial abnormalities in Alzheimer's disease. *J Neurosci* **21**, 3017-3023.

[56] Yudkoff M, Daikhin Y, Horyn O, Nissim I (2008) Ketosis and brain handling of glutamate, glutamine, and GABA. *Epilepsia* **49**, 73-75.

[57] Henderson ST (2013) Targeting diminished cerebral glucose metabolism for Alzheimer's disease. *Drug Discov World* **14**, 16-20.